

Electrical Power Quality and Utilisation, Journal Vol. XIII, No. 1, 2007

The Effect of the Integration Interval on the Measurement Accuracy of RMS Values and Powers in Systems with Nonsinusoidal Waveforms

Lorenzo PERETTO ¹⁾, Jacques L. WILLEMS ²⁾ and Alexander E. EMANUEL ³⁾

1) Dipartimento di Ingegneria Elettrica, Alma Mater Studiorum, Università di Bologna, Italy

2) Engineering Faculty, Ghent University, Belgium

3) Department of Electrical and Computer Engineering, Worcester Polytechnic Institute, USA

Summary: In this paper the possibility of errors in the measurement of average values (in particular rms values or active powers) in power systems under nonsinusoidal conditions are discussed. The errors considered are either due to the fact that the measurement time interval is not an exact multiple of the fundamental period of the voltage and current signals, or due to the presence of interharmonics or subharmonics. The errors are calculated and the results are illustrated by means of simple examples.

1. INTRODUCTION

The ideal and idealized operation of an a.c. power system corresponds to sinusoidal voltages and currents with a frequency of 50 Hz or 60 Hz. However in real situations there are deviations from this ideal case. The steady-state operation of electrical loads containing power electronics devices gives rise to current and/or voltage signals that feature a discrete spectrum and can be periodic (with a period usually far longer than 20 ms, which in the European Union corresponds to the industrial frequency) or even non-periodic. Interesting theoretical and technical issues must therefore be tackled in the design and implementation of measurement systems for the monitoring and diagnostics of the above equipments. In the case in which the discrete spectrum signal features spectral components not harmonically related each other, then it is referred to as *multi-tone signal*. Furthermore, when some spectral components are also non-commensurable with respect to some others, then the signal is non periodic and referred to as *almost-periodic* [1–5].

Let us consider an electric power system in a given state. Once the spectral components of the voltage and current signals are known, any quantity providing significant information on the system properties and behavior can be measured. This way, monitoring and diagnostics tasks can be tackled. In the case of a periodic signal, the spectral analysis can easily be performed by applying the Discrete Fourier Transform (DFT) to a sequence of data acquired at regular time intervals over a measurement interval multiple of the signal period. If the signal is periodic, the sampling process can be synchronous or asynchronous with the signal period; as for the latter case, the acquisition process can also be based on a random strategy. In this case, the sampling frequency could even be lower than the signal frequency (this turns into an equivalent time sampling). As the number of processed samples increases, the estimates of the signal spectral components converge to the actual ones. In the case of quasi-periodic signals, or periodic multi-tone signals having

a period much greater than the measurement interval, the requirements for the application of the DFT algorithm are not met, given that the measurement time interval does not match the requirement of being multiple of the signal period. This leads to a significant distortion of the signal spectrum, due to the presence of side lobes of the rectangular window function representing the measurement time interval. This way, the energy of the generic component resulting from the DFT application is distributed over all the other components determined. This effect is known as *spectral leakage*.

Several Digital Signal Processing (DSP) techniques, which apply DFT algorithms to finite-length non-periodic sequences of acquired data, have been proposed in the literature to overcome this limitation [3, 14, 15, 16]. They can be grouped into two main categories: windowing and statistical techniques. If the requirements of the sampling theorem are met, windowing allows the reduction of the above limitations by multiplying the digital signal with a non rectangular function which exhibits low side-lobe levels. For instance the common Hanning or Hamming windows fulfill the above characteristics. When random sampling strategies are implemented, and statistical techniques are used to process the acquired data, the sampling instants must be properly chosen. These methods, if compared to deterministic approaches, require processing a much greater amount of data. However, statistical approaches allow to overcome the sampling theorem and, hence, to avoid aliasing and leakage [6].

In the present paper the measurements errors are analyzed which are due to:

- the fact that the measurement interval is not an exact multiple of the signal period for periodic signals,
- the presence of interharmonics which are the cause that the signal is not exactly periodic.

In Section 3 the measurement of rms values and power is discussed. General expressions for the errors introduced by the above phenomena on the measurement of rms values and of (average) powers are derived. The results are illustrated by means of simple examples.

2. DEFINITIONS OF RMS VALUE AND POWERS AND THEIR IMPLEMENTATION

$$S = VI \quad (4)$$

and the active power as:

$$P = \frac{1}{T_m} \int_0^{T_m} v i dt = \sum_h V_h I_h \cos(\alpha_h - \beta_h) \quad (5)$$

2.1. Definitions

International Standards endorse definitions and prescriptions on how to measure rms values and active, non-active and apparent powers in power systems with periodic voltages and currents.

Let:

$$\begin{aligned} v &= \sum_h \hat{V}_h \sin(h\omega t + \alpha_h) \\ i &= \sum_h \hat{I}_h \sin(h\omega t + \beta_h) \end{aligned} \quad (1)$$

with $h = 1, 2, 3, \dots$, be the expressions of the voltage and current in an electric system represented according to the Fourier representation. In (1) $\omega = 2\pi f = 2\pi/T$, with f and T the fundamental frequency and period. \hat{V}_h and \hat{I}_h represent the amplitudes of the voltage and current spectral components, $V_h = \hat{V}_h/\sqrt{2}$ and $I_h = \hat{I}_h/\sqrt{2}$ their rms values. α_h and β_h their phase angles, and h the corresponding harmonic order. The rms values of the voltage and the current are given by:

$$V^2 = \sqrt{\frac{1}{T_m} \int_0^{T_m} v^2 dt} = \sqrt{\sum_h V_h^2} \quad (2)$$

and:

$$I^2 = \sqrt{\frac{1}{T_m} \int_0^{T_m} i^2 dt} = \sqrt{\sum_h I_h^2} \quad (3)$$

In these expressions T_m is the integration time, which represents the signal observation or measurement time interval. In the present case, it is assumed to be an integer multiple of the fundamental period T of the current and voltage.

The apparent power is defined as:

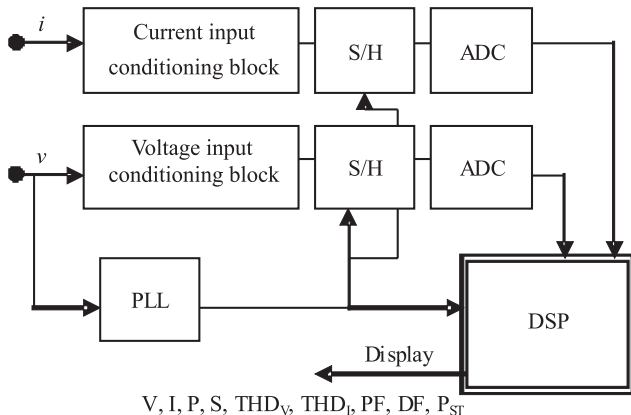


Fig.1. Schematic block diagram of a single-phase power meter

2.2. Architecture of the modern power meters

Figure 1 represents the single-phase schematic block diagram of typical modern power meter. Voltage and current analog conditioning blocks provide both suitable amplification or attenuation of input signals and anti-aliasing filters for being correctly acquired and converted by the Sample & Hold device (S/H) and the analog to digital converter (ADC) devices.

Usually the sampling frequency is less than 10 kSa/s per channel for rms or power measurements. The analog-to-digital converters feature a resolution of 12 to 16 bits. On-the-market power meters feature generally different measurement functions: rms values, powers, power factors (PF), displacement factors (DF), flicker severity (P_{ST}), harmonic analysis, swells, sags, transients and so on. For transients detection usually the sampling frequency rises up to some MSa/s. The PLL block allows both the measurement time interval to be set as multiple of the signal period and the sampling frequency to be multiple of the fundamental frequency in order to avoid leakage effect when calculating all average quantities. According to [8] the PLL frequency can feature an accuracy of 0.03% of the system frequency, while instruments including a PLL shall meet the requirements for accuracy and synchronisation for measuring at any signal frequency within a range of at least 5% of the nominal system frequency.

According to [9] the measurement time interval for rms values must be a 10-cycle time interval for 50 Hz power systems or a 12-cycle time interval for 60 Hz power systems. The value of the measurement time interval is obtained by performing the mean of the number of cycles over a 10s time interval. This value is used for the derivation of all the average quantities.

3. THE EFFECT OF THE MEASUREMENT TIME ON RMS AND POWER MEASUREMENTS

The result of the measurement of physical quantities performed by modern instrumentation can be affected by the contribution of several sources of uncertainty. According to the "Guide to the Expression of Uncertainty in Measurements" [10], two distinct evaluation types have to be used for evaluating the uncertainty affecting a measurement results: Type A and Type B evaluation. Each of them takes into account distinct sources of uncertainty. Hence both the evaluation methods must be implemented for a complete knowledge of the uncertainty affecting a measurement reading. As far as the Type A evaluation method is concerned, it quantifies the contribution to the uncertainty due to all the random contributions, like noise, disturbances,

temperature, etc. This evaluation method requires a given number of measurements to be obtained and is based on a statistical analysis of the acquired data for characterizing the uncertainty in terms of the standard deviation. As far as the Type B evaluation mode is concerned, it uses the typical indexes provided by the instrument's manufacturer (“%reading” and “%range”, “offset”) for evaluating the relevant uncertainty contributions. The contributions provided by both methods are to be added to obtain the so called *composite standard uncertainty*. This uncertainty is due to both the instrument limits and the interaction of the instrument itself with the environment surrounding the test bench.

In the measurement of average quantities, like rms values, active, nonactive or apparent powers, further contributions to the uncertainty affecting the measurement results can arise from the lack of knowledge of the characteristics of the input quantities or from a wrong setting of the instrument parameters or from a non-ideal behavior of some devices. In such cases the deviation of the measurement results from the right value is not referred to as *uncertainty* but as *error*.

Two distinct error sources can be distinguished:

1. The measurement time interval is not exactly equal to a multiple of the signal period. This can be due either to a wrong instrument setting or to the uncertainty affecting the PLL frequency. As reported in Section 2, such an effect is referred to as *spectral leakage*.
2. The real signal period is not the inverse of the fundamental frequency (50 Hz or 60 Hz) due to the presence of interharmonics or subharmonics. In such a case the actual signal period is indeed different from the period corresponding to the fundamental frequency. The inner PLL does not lock to the signal period, but it continues to lock to the inverse of the frequency of 50 Hz or 60 Hz. As a consequence the instrument readings swing.

In the sequel the analysis of the effect of such error sources on the measurement of rms values and (average) powers is presented and discussed.

3.1. Error on rms measurements

3.1.1. The measurement time interval is not an exact multiple of the signal period.

Let us consider the simple case of a sinusoidal voltage

$$v(t) = \hat{V} \sin(\omega t) \quad (6)$$

with \hat{V} the peak value. In the case that the measurement time T_m is not an exact multiple of the fundamental period $T = 2\pi/\omega$, the expression of the measured value of the square of the rms voltage is:

$$\begin{aligned} V_{meas}^2 &= \frac{1}{T_m} \int_0^{T_m} [\hat{V} \sin(\omega t)]^2 dt = \frac{\hat{V}^2}{T_m} \int_0^{T_m} \sin^2(\omega t) dt = \\ &= \frac{1}{2} \hat{V}^2 \left(1 - \frac{\sin(2\omega T_m)}{2\omega T_m} \right) \end{aligned} \quad (7)$$

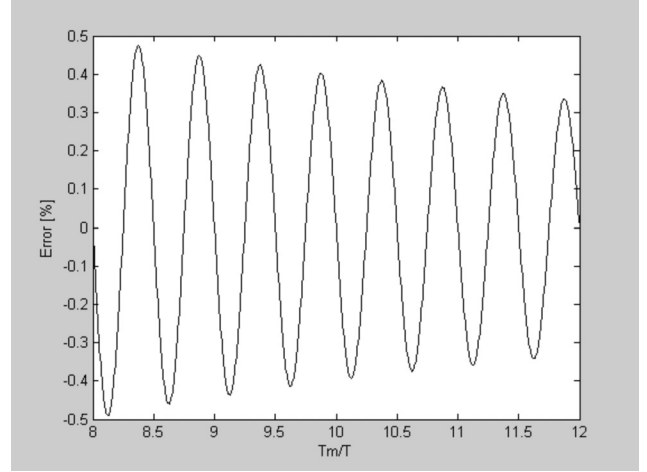


Fig. 2. Error $\% \varepsilon_V$ on the rms value vs. the ratio T_m/T

The value of the error on the square of the rms value is:

$$\varepsilon_{V_{meas}^2} = -\hat{V}^2 \frac{\sin(2\omega T_m)}{4\omega T_m} \quad (8)$$

An approximation of the error on the rms voltage can be obtained by developing (7) according to the Taylor series. We obtain:

$$V_{meas} = \sqrt{\frac{1}{2} \hat{V}^2 \left(1 - \frac{\sin(2\omega T_m)}{2\omega T_m} \right)} \cong \sqrt{\frac{1}{2}} \hat{V} \left(1 - \frac{\sin(2\omega T_m)}{4\omega T_m} \right) \quad (9)$$

The (approximate) relative error with respect to the actual rms voltage V is hence:

$$\begin{aligned} \% \varepsilon_V &= 100 \cdot \frac{V_{meas} - V}{V} \% \cong -100 \cdot \frac{\sin(2\omega T_m)}{4\omega T_m} \% = \\ &= -100 \cdot \frac{\sin(4\pi T_m / T)}{8\pi T_m / T} \% \end{aligned} \quad (10)$$

Figure 2 plots the error, as given by (10), vs. the ratio T_m/T . The plot clearly shows that $\% \varepsilon_V$ decreases if the ratio T_m/T increases.

3.1.2. Nonharmonic components present in the signal.

Now we analyze the effect of the presence of a nonharmonic component. For simplicity we assume that the signal only contains a fundamental component and a nonharmonic component:

$$v(t) = \hat{V} \sin(\omega t) + \hat{V}_s \sin(s\omega t + \alpha_s) \quad (11)$$

where s is a non-integer which may be larger or smaller than 1. \hat{V}_s is the peak value of the nonharmonic component. Under the assumption that the measurement time interval T_m is exactly a multiple of the fundamental period T , $T_m = mT$, the expression of the square of the voltage rms, is:

$$\begin{aligned}
V^2 &= \frac{1}{T_m} \int_0^{T_m} [\hat{V} \sin(\omega t) + \hat{V}_s \sin(s\omega t + \alpha_s)]^2 dt = \quad (12) \\
&= \frac{1}{T_m} \int_0^{T_m} [\hat{V}^2 \sin^2(\omega t) + \hat{V}_s^2 \sin^2(s\omega t + \alpha_s) + 2\hat{V}\hat{V}_s \sin(\omega t) \sin(s\omega t + \alpha_s)] dt = \\
&= \frac{\hat{V}^2}{2} + \frac{\hat{V}_s^2}{2} \int_0^{T_m} \left(\frac{1}{2} - \frac{1}{2} \cos(2s\omega t + 2\alpha_s) \right) dt + \\
&+ \frac{2\hat{V}\hat{V}_s}{T_m} \int_0^{T_m} \left(\frac{1}{2} \cos[(1-s)\omega t - \alpha_s] \right) dt - \frac{2\hat{V}\hat{V}_s}{T_m} \int_0^{T_m} \left(\frac{1}{2} \cos[(1+s)\omega t + \alpha_s] \right) dt = \\
&= \frac{\hat{V}^2}{2} + \frac{\hat{V}_s^2}{2} + \frac{\hat{V}_s^2}{2} \frac{\sin(2\alpha_s) - \sin(2s\omega T_m + 2\alpha_s)}{2s\omega T_m} + \\
&+ 2\hat{V}\hat{V}_s \frac{\sin[(1-s)\omega T_m - \alpha_s] + \sin \alpha_s}{(1-s)\omega T_m} - 2\hat{V}\hat{V}_s \frac{\sin[(1+s)\omega T_m + \alpha_s] - \sin \alpha_s}{(1+s)\omega T_m}
\end{aligned}$$

The exact value of the square of the voltage rms value is:

$$V^2 = \frac{\hat{V}^2}{2} + \frac{\hat{V}_s^2}{2}$$

The measurement error is hence:

$$\begin{aligned}
&\frac{\hat{V}_s^2}{2} \frac{\sin(2\alpha_s) - \sin(2s\omega T_m + 2\alpha_s)}{2s\omega T_m} + \hat{V}\hat{V}_s \frac{\sin[s\omega T_m - \alpha_s] + \sin \alpha_s}{(s-1)\omega T_m} - \\
&- \hat{V}\hat{V}_s \frac{\sin[s\omega T_m + \alpha_s] - \sin \alpha_s}{(s+1)\omega T_m} = -\frac{\hat{V}_s^2}{2} \frac{\sin(sm2\pi) \cos(sm2\pi + 2\alpha_s)}{sm2\pi} + \quad (13) \\
&+ 2\hat{V}\hat{V}_s \frac{\sin[sm\pi] \cos[s]m\pi + \alpha_s}{(s-1)m2\pi} - 2\hat{V}\hat{V}_s \frac{\sin[sm\pi] \cos[s]m\pi + \alpha_s}{(s+1)m2\pi}
\end{aligned}$$

From this expression the expression of the relative error can readily be derived.

In practical situations the nonharmonic component may be assumed to be much smaller than the fundamental component. Then the relative error on the rms voltage may be approximated by:

$$\% \varepsilon_V \equiv 100 \frac{2\hat{V}_s}{\hat{V}} \left(\frac{\sin(sm\pi) \cos(sm\pi + \alpha_s)}{(s-1)m2\pi} - \frac{\sin(sm\pi) \cos(sm\pi + \alpha_s)}{(s+1)m2\pi} \right) \% \quad (14)$$

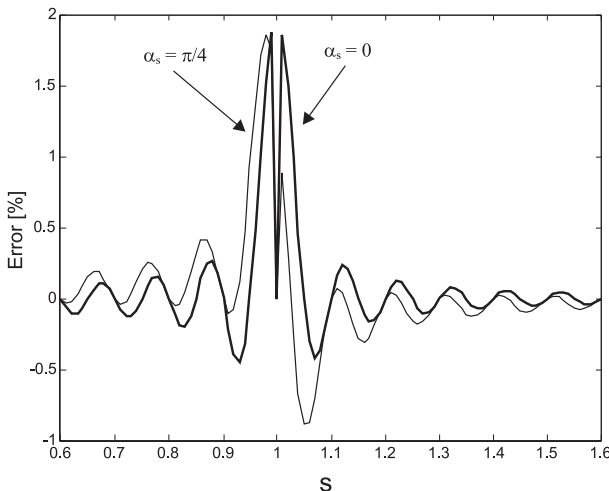


Fig. 3. Error term vs. s

This expression shows that the largest error is obtained when the nonharmonic frequency is close to the fundamental frequency. Around $s = 1$ the relative error is approximately given by:

$$\frac{\hat{V}_s}{\hat{V}} \cos \alpha_s$$

To illustrate the measurement error, we consider the numerical case where the peak value of the nonharmonic is 2% of the peak value of the fundamental (as typically occurs in actual conditions, see e.g. [12]), and the measurement time interval is 10 times the fundamental period ($m = 10$). Figure 3

plots the trend of $\% \varepsilon_V$ vs. s for $\alpha_s = 0$ and $\alpha_s = \frac{\pi}{4}$. We note

that the error reaches approximately the 2%, equal to the relative amplitude of the nonharmonic component. It can be seen also from (14) that the error is directly proportional to the amplitude of the nonharmonic component.

3.2. Error on power measurement

As in the case of the rms measurement, we separately analyze the measurement error due to a measurement time different from a multiple of the fundamental period T and the measurement error due to the presence of inter- or subharmonics. In both cases the relative error can be expressed by the following index:

$$\% \varepsilon = 100 \cdot \frac{P_{meas} - P}{S} \% \quad (15)$$

with P the actual power, P_{meas} the measured power and S the apparent power.

3.2.1. The measurement time is not an exact multiple of the signal period.

For the sake of simplicity but without loss of generality, let us assume that voltage and current are sinusoidal. Then the expression of the measurement of the active power is:

$$\begin{aligned}
P_{meas} &= \frac{1}{T_m} \int_0^{T_m} \hat{V} \hat{I} \sin(\omega t + \alpha) \sin(\omega t + \beta) dt = \\
&= \frac{\hat{V}\hat{I}}{2} \cos(\beta - \alpha) - \frac{\hat{V}\hat{I}}{4\omega T_m} [\sin(2\omega T_m + \alpha + \beta) - \sin(\alpha + \beta)] = \quad (16) \\
&= \frac{\hat{V}\hat{I}}{2} \cos(\beta - \alpha) - \frac{\hat{V}\hat{I}}{2\omega T_m} \sin(\omega T_m) \cos(\omega T_m + \alpha + \beta)
\end{aligned}$$

The expression of the relative error, as defined by (15), is:

$$\begin{aligned}
\% \varepsilon &= -100 \cdot \frac{\sin(4\pi T_m / T + \alpha + \beta) - \sin(\alpha + \beta)}{4\pi T_m / T} \% = \\
&= -100 \cdot \frac{\sin(2\pi T_m / T) \cos(2\pi T_m / T + \alpha + \beta)}{2\pi T_m / T} \% \quad (17)
\end{aligned}$$

Expression (17) shows that the relative error $\% \varepsilon$ depends on the phase angles of the voltage and the current and

decreases as the measurement time T_m increases. The error is obviously zero if the measurement time interval is a multiple of the fundamental period. The error oscillates when T_m increases, and reaches maximal positive and negative values in the vicinity of the measurement time intervals for which $4\pi T_m / T + \alpha + \beta$ is a multiple of $\pi/2$. The largest positive and negative errors are obtained if $\alpha + \beta$ have values corresponding respectively to $2k\pi + \frac{\pi}{2}$ or $2k\pi - \frac{\pi}{2}$. In these cases the largest errors are obtained when the measurement interval deviates from a multiple of the fundamental period by a quarter of that period. Figure 4 shows a plot of the error for $\alpha + \beta$ equal to $\pi/2$ (worst case – largest positive errors) and equal to 0.

3.2.2. Non-harmonic components present in the voltage and the current.

To analyze this case the following expressions are taken for the voltage and current:

$$\begin{aligned} v(t) &= \hat{V} \sin(\omega t + \alpha) + \hat{V}_s \sin(s\omega t + \alpha_s) \\ i(t) &= \hat{I} \sin(\omega t + \beta) + \hat{I}_s \sin(s\omega t + \beta_s) \end{aligned} \quad (18)$$

where $s\omega$ is the angular frequency of a non-harmonic component of voltage and current of amplitudes \hat{V}_s and \hat{I}_s with phases α_s and β_s , respectively. In this case the expression of the corresponding active power is:

$$\begin{aligned} P_{meas} &= \frac{1}{T_m} \int_0^{T_m} \hat{V} \hat{I} \sin(\omega t + \alpha) \sin(\omega t + \beta) dt + \\ &+ \frac{1}{T_m} \int_0^{T_m} \hat{V}_s \hat{I} \sin(s\omega t + \alpha_s) \sin(\omega t + \beta) dt + \\ &+ \frac{1}{T_m} \int_0^{T_m} \hat{V} \hat{I}_s \sin(\omega t + \alpha) \sin(s\omega t + \beta_s) dt + \\ &+ \frac{1}{T_m} \int_0^{T_m} \hat{V}_s \hat{I}_s \sin(s\omega t + \alpha_s) \sin(s\omega t + \beta_s) dt \end{aligned} \quad (19)$$

Under the assumption that $T_m = kT$, with k integer, the result is:

$$\begin{aligned} P_{meas} &= \frac{\hat{V} \hat{I}}{2} \cos(\alpha - \beta) + \frac{\hat{V}_s \hat{I}}{2} \frac{\sin((s-1)\omega T_m + \alpha_s - \beta) - \sin(\alpha_s - \beta)}{(s-1)\omega T_m} \\ &- \frac{\hat{V}_s \hat{I}}{2} \frac{\sin((s+1)\omega T_m + \alpha_s + \beta) - \sin(\alpha_s + \beta)}{(s+1)\omega T_m} + \\ &+ \frac{\hat{V} \hat{I}_s}{2} \frac{\sin((1-s)\omega T_m + \alpha - \beta_s) - \sin(\alpha - \beta_s)}{(1-s)\omega T_m} - \\ &- \frac{\hat{V} \hat{I}_s}{2} \frac{\sin((1+s)\omega T_m + \alpha + \beta_s) - \sin(\alpha + \beta_s)}{(1+s)\omega T_m} + \frac{\hat{V}_s \hat{I}_s}{2} \cos(\alpha_s - \beta_s) - \\ &- \frac{\hat{V}_s \hat{I}_s}{2} \frac{\sin(2s\omega T_m + \alpha_s + \beta_s) - \sin(\alpha_s + \beta_s)}{2s\omega T_m} \end{aligned} \quad (20)$$

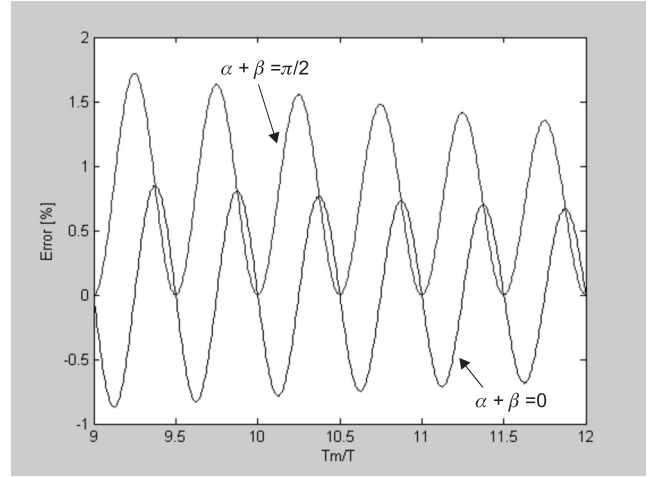


Fig.4. Error %e vs. T_m/T with $a+b = \pi/2$ (worst case) and $a+b = 0$

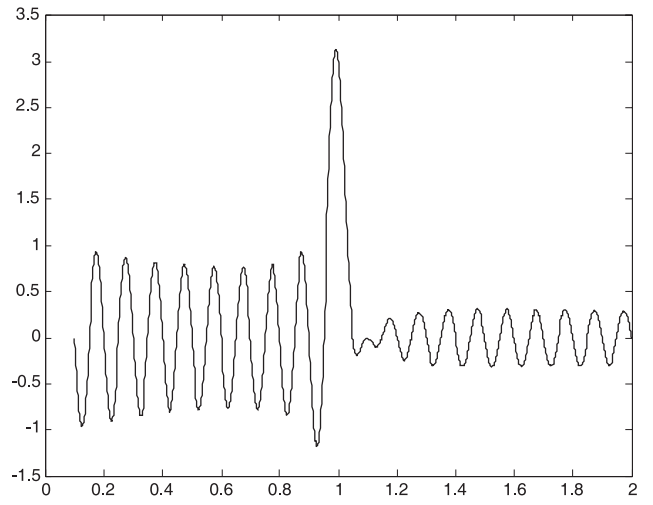


Fig. 5. Error %e vs. s in the range [0-2]

The correct value of the active power is:

$$P = \frac{\hat{V} \hat{I}}{2} \cos(\alpha - \beta) + \frac{\hat{V}_s \hat{I}_s}{2} \cos(\alpha_s - \beta_s)$$

From (20) it is clear that a measurement error occurs if the measurement time interval is not a multiple of the period of the interharmonic or subharmonic components. Let us assume that the amplitudes of the voltage and current fundamental are much larger than the amplitudes of the interharmonic of the voltage and the current respectively. Taking into account that ωT is a multiple of 2π , the error can hence be approximated by:

$$\begin{aligned} \%e &= 100 \cdot \frac{P_{meas} - P}{P} \% \approx 100 \frac{\hat{V}_s}{\hat{V}} \frac{\sin(s\omega T_m + \alpha_s - \beta) - \sin(\alpha_s - \beta)}{(s-1)\omega T_m} \% - \\ &- 100 \frac{\hat{V}_s}{\hat{V}} \frac{\sin(s\omega T_m + \alpha_s + \beta) - \sin(\alpha_s + \beta)}{(s+1)\omega T_m} \% + \\ &+ 100 \frac{\hat{I}_s}{\hat{I}} \frac{\sin(-s\omega T_m + \alpha - \beta_s) - \sin(\alpha - \beta_s)}{(1-s)\omega T_m} \% - \\ &- 100 \frac{\hat{I}_s}{\hat{I}} \frac{\sin(s\omega T_m + \alpha + \beta_s) - \sin(\alpha + \beta_s)}{(1+s)\omega T_m} \% \end{aligned} \quad (21)$$

Figure 5 shows the relative error for s in the range $[0, 2]$, if the interharmonics of the voltage is assumed to be 1% and 2% of the corresponding fundamental components, respectively, (as typically occurs in actual conditions, see e.g. [12]), and if all phase angles are assumed to be zero. The measurement time interval T_m is assumed to be equal to $10T$. As in subsection 4.1.2 the largest error occurs when the subharmonic or interharmonic has a frequency close to the fundamental frequency. Then an error of approximately 3% may occur if the subharmonics or interharmonics in the current and the voltage are 2% and 1%, respectively, of the fundamental components. As stated in Section 4.1.2 the error is directly proportional to the sum of amplitudes of the nonharmonic components.

5. CONCLUSIONS

This paper deals with the measurement of average values (in particular rms values or active powers) in the case of nonsinusoidal periodic voltage and current waveforms. It was shown that errors can be introduced in these measurements. It was pointed out that these errors may be caused by two reasons:

1. A measurement error is introduced if the measurement time interval is not an exact multiple of the fundamental period of the voltage and current signals.
2. A measurement error may be due to the presence of interharmonics or subharmonics in the voltage and/or current signals.

The errors have been analyzed and explicitly calculated. The results have been illustrated by means of simple examples.

It is clear that the examples, which have been presented in this paper, are simple cases. However they are sufficient to show why and how the above measurement errors arise. In the general case, with the presence of more harmonics, interharmonics and subharmonics, the two sources of errors simultaneously lead to measurement errors, caused by the fundamental component and all other components and their mutual interactions. The analysis of these more general cases however does not yield essential new phenomena.

REFERENCES

1. Bohr H.: *Fastperiodische Funktionen*. Erg. Math., Berlin, Germany, Springer, 1932.
2. Carbone P., Nunzi E. and Petri D.: *Sampling criteria for the estimation of multisine signal parameters*. Proc. IEEE IMTC/2000, Baltimore (USA), Vol. 2, pp. 636–640, 2000.
3. Andria G., Savino M., and Trotta A.: *FFT-based algorithms oriented to measurements on multifrequency signals*. Measurement, Vol. 12, no. 1, pp. 25–42, 1993.
4. Ushida A., and Chua L.O.: *Frequency domain analysis of nonlinear circuits driven by multi-tone signals*. IEEE Trans. on Circuits and Systems, Vol. 31, pp.766–778, 1984.
5. Itô K. (Editor): *Encyclopedic dictionary of mathematics*. The Mathematical Society of Japan, Cambridge (USA), MIT Press, 1987.
6. Peretto L., Staudt V., Sasdelli R., and Tinarelli R.: *Performance Comparison of a Deterministic and Statistical Approach for the Analysis of a Multi-Tone Signal*. 3rd IEEE Symposium on Diagnostics for Electrical Machines, Power Electronics and Drives (SDEMPED '01), Grado, Italy, September 2001, pp. 325–331.

7. IEEE Std. 1459: *Definitions for the measurement of electric quantities under sinusoidal, nonsinusoidal, balanced, or unbalanced conditions*. Institution of Electrical and Electronics Engineers, Jan. 2000.
8. BS EN 61000-4-7: *Electromagnetic Compatibility – Part 4-7: Testing and measurement techniques – General guide on harmonics and interharmonics measurements and instrumentation, for power supply systems and equipment connected thereto*. 2003.
9. BS EN 61000-4-30: *Electromagnetic Compatibility – Part 4-30: Testing and measurement techniques Power quality measurement methods*. 2003.
10. EN 13005: *Guide to the expression of uncertainty in measurement*. 1999.
11. EN 50160: *Voltage characteristics of electricity supplied by public distribution systems*. 2004.
12. IEEE Std. 519: *IEEE Recommended Practices and Requirements for Harmonic Control in Electrical Power Systems*. Institution of Electrical and Electronics Engineers, 1993.
13. Peretto L., Sasdelli R.: *Measurements for the characterization of quasi-periodic waveforms*. ETEP, Eur. Trans. on Electr. Power, vol. 12, no. 1, 2002, pp. 11–16.
14. Borkowski J.: *LIDFT-the DFT linear interpolation method*. IEEE Trans. Inst. Meas., vol. 49, No. 4, Aug. 2000, pp. 741–745.
15. Fusheng Z., Zongxing G. and Wei Y.: *The algorithm of interpolating windowed FFT for harmonic analysis of electric power system*. IEEE Trans. Power Del., vol. 16, No. 2, Apr. 2001, pp. 160–164.
16. Staudt V., Wiesemann J.: *Identification of sinusoidal functions contained in a signal*. in Proc. of IEEE ICHQP VII, Las Vegas, USA, 1996, pp. 375–380.



Lorenzo Peretto (M'98) (SM'03)

received the laurea degree in electronic engineering and the Ph.D. degree in electrical engineering from the University of Bologna, Italy, in 1993 and 1997, respectively. In 1998 he joined the Department of Electrical Engineering of the University of Bologna as an Assistant Professor with the Electrical and Electronic Measurement Group and since January 2004 as an Associate Professor. His fields of research are

digital signal processing, measurements for the analysis of Power Quality, distributed measurement instrumentation; design of new electromagnetic-fields sensors and instrumentation; reliability prediction electronic systems;

Address:

Department of Electrical Engineering,
University of Bologna,
Viale Risorgimento 2, Bologna, Italy.
e-mail: lorenzo.pereto@mail.ing.unibo.it
tel.: +39 051 20 93483, fax: +39 051 20 93588



Jacques L Willems

(Fellow IEEE) was born in Bruges, Belgium, on September 18, 1939. He graduated in electromechanical engineering from Ghent University, Belgium, and received the Master of Science degree from M.I.T. and the doctoral degree from Ghent University.

Since 1964 he has been with the Engineering Faculty of Ghent University, teaching and doing research in the areas of power system analysis and control theory. He was a Visiting Research Fellow at Harvard University in 1970 and Professeur Visiteur at the Université Nationale du Rwanda in 1982. He was Dean of the Engineering Faculty from 1988 tot 1992 and Rector of Ghent University from 1993 tot 2001.

The research was partially supported by the Belgian Programme of Interuniversity Attraction Poles, initiated by the Belgian State, Prime Minister's Office for Science, Technology and Culture. The scientific responsibility rests with the author.

Address:

Department EESA, Ghent University,
Technologiepark-Zwijnaarde, 914, B-9052 Gent, Belgium.
e-mail: Jacques.Willems@UGent.be,
tel.: +32-9-2645648, fax: +32-9-2645840



Alexander E. Emanuel (SM'1970, F'94, LF'05)

was born in Bucuresti, Rumania. He earned B.Sc, M.Sc and D.Sc. in 1963, 65 and 69, all from Technion, Israel Institute of Technology. From 1969 till 1974 he was employed by High Voltage Engineering where he helped design and test SF6 insulated cables and shunt reactances. In 1974 he joined Worcester Polytechnic Institute where presently is a Professor of Electrical and Computer Engineering. His research interest is quality of electric energy, power electronics and design of power equipment.

Address:

Department of Electrical and Computer Engineering,
Worcester Polytechnic Institute,
100 Institute Road, Worcester, MA 01609-2280, USA
e-mail: aemanuel@ece.wpi.edu
tel.: +15 08 831 5231, fax: +15 08 831 5491